

# Magnetic Induction-Based Localization in Randomly-Deployed Wireless Underground Sensor Networks

Shih-Chun Lin, *Member, IEEE*, Abdallah Awadh Alshehri, Pu Wang, *Member, IEEE*, and Ian F. Akyildiz, *Fellow, IEEE*

**Abstract**—Wireless underground sensor networks enable many applications, such as mine and tunnel disaster prevention, oil upstream monitoring, earthquake prediction and landslide detection, and intelligent farming and irrigation among many others. Most applications are location-dependent, so they require precise sensor positions. However, classical localization solutions based on the propagation properties of electromagnetic waves do not function well in underground environments. This paper proposes a magnetic induction (MI)-based localization that accurately and efficiently locates randomly-deployed sensors in underground environments by leveraging the multi-path fading free nature of MI signals. Specifically, the MI-based localization framework is first proposed based on underground MI channel modeling with additive white Gaussian noise, the designated error function, and semidefinite programming relaxation. Next, the paper proposes a two-step positioning mechanism for obtaining fast and accurate localization results by: first, developing the fast-initial positioning through an alternating direction augmented Lagrangian method for rough sensor locations within a short processing time, and then proposing fine-grained positioning for performing powerful search for optimal location estimations via the conjugate gradient algorithm. Simulations confirm that our solution yields accurate sensor locations with both low and high noise and reveals the fundamental impact of underground environments on the localization performance.

**Index Terms**—Wireless underground sensor network, magnetic induction communication, localization algorithms, semidefinite programming (SDP), alternating direction augmented Lagrangian method (ADM), conjugate gradient algorithm (CGA).

## I. INTRODUCTION

**W**IRELESS underground sensor networks (WUSNs) are a network of wirelessly-interconnected sensor nodes deployed in a variety of underground environments, such as soil, underground tunnels, and oil reservoir [1]. They can enable a wide range of emerging applications, such as mine and tunnel disaster prevention, oil gas extraction, underground power grid monitoring, earthquake and landslide forecast, border patrol and security, intelligent irrigation, and etc. Most

This research was supported by the US National Science Foundation (NSF) under Grant No. 1320758.

S.-C. Lin is with the Department of Electrical and Computer Engineering, North Carolina State University, Raleigh, NC 27606, USA (e-mail: slin23@ncsu.edu). A. A. Alshehri and I. F. Akyildiz are with the Broadband Wireless Networking Laboratory, School of Electrical and Computer Engineering, Georgia Institute of Technology, Atlanta, GA 30332, USA (email: aalshehri9@ece.gatech.edu; ian@ece.gatech.edu). P. Wang is with the Department of Computer Science, the University of North Carolina at Charlotte (email: Pu.Wang@uncc.edu).

of the applications, in particular, in oil reservoir digging, require the knowledge of location information of the randomly deployed sensor nodes. However, the challenged underground environments prevent the direct application of the conventional localization solutions based on the propagation properties of electromagnetic (EM) waves because of the extremely short communication ranges, highly unreliable channel conditions, and large antenna sizes [2].

Magnetic induction (MI)-based underground communication is a promising wireless communication solution [3], [4] that utilizes time-varying magnetic fields to deliver the information in challenged underground environments, including soil, oil reservoir, and underground water pipelines. Different from conventional EM-based communication, MI-based communication exhibits highly reliable and constant channel conditions with sufficiently large communication ranges in underground [5]–[7]. First, contrary to EM waves, whose performance is highly dependent on numerous environmental properties such as water contents, soil makeup (i.e., sand, silt, or clay) and density, and specific crude oil composition, underground mediums (such as soil, sand, water, and crude oil) cause little variation in the attenuation rate of magnetic fields from that of air, due to similar magnetic permeability of each of these mediums [5]. Second, the multi-path fading is negligible in underground MI systems [6], because communication ranges in these systems are within one wavelength and even if there exist multiple paths between the transceivers, the phase shifting of multiple paths is so small that the coherence bandwidth is much larger than the system bandwidth. Third, large-size antennas are necessary for efficient propagations of EM waves in underground environments, since the path loss of low frequency signal is small. However, large antenna sizes make underground sensors impractical. In MI-based communication, the transmission and reception are accomplished via small-size wire coils. There is no cutoff frequency as in the EM wave-based technique [7]. Hence, small coil antennas are enough for MI-based communication and low frequency signals.

In this paper we propose a novel MI-based localization solution, which utilizes the promising features of MI channel and the byproduct of MI-based communication, i.e., received magnetic field strength (RMFS), to guarantee the accuracy, simplicity, and convenience of the localization strategy. To the best of our knowledge, this work is the first optimized localization solution for WUSNs. Specifically, by leveraging the unique multi-path fading free and highly constant prop-

erties of MI channel [5], [6], we derive the mutual distance estimation between sensor nodes in such AWGN channels. Note that this AWGN modeling is validated through several experiments of MI-based communication in an underground in-lab testbed [8]. Next, based on such distance estimations, we propose a MI-based localization framework by formulating it as a semidefinite programming (SDP) relaxation problem with the designated error function. In particular, the error function depicts the mismatch between actual and estimated transmission distances, and SDP relaxation further reformulates the error minimization into a convex relaxation problem for accurate sensor positioning. To realize the introduced framework, two successive positioning algorithms are proposed for fast and accurate localization. In particular, a fast-initial positioning scheme is first proposed through alternating direction augmented Lagrangian method (ADM) [9] to obtain rough sensor locations within short processing time. To improve the accuracy of the initial positioning results, a fine-grained positioning solution is then proposed through conjugate gradient algorithm (CGA) [10] to perform powerful search for optimal location estimations.

It is worth to note that the SDP relaxation and optimization scheme has been applied in solving terrestrial localization problem [11]. However, this scheme suffers from a poor convergence speed and therefore is not suitable for large-scale underground sensor networks. The reason is that it does not explore the inherited optimization structure and therefore can be only solved by the conventional primal-dual convex optimization tool (e.g., SeDuMi [12]). By our solution, we intentionally exploit the proposed localization problem structure by transforming the SDP relaxation formulation into a suitable format in such way that it is solvable via a fast-convergent algorithm, i.e., alternating direction augmented Lagrangian method (ADM) [9] that has recently been used to provide a powerful leverage for the algorithm analysis resulted from convex relaxation. What is more important, all the existing localization solutions fail to address the unique challenges faced by wireless channels in underground environments, which will inevitably induce high localization errors if without proper underground channel modeling. Towards this, our proposed localization solution jointly applies ADM and CGA with regards of MI-based communication channel to achieve high positioning accuracy in WUSNs, while maintaining high computational efficiency.

The major contributions of this paper are as follows:

- 1) By using a limited number of two anchors we conduct received magnetic field strength measurements and introduce a localization algorithm based on error function and semidefinite programming relaxation for underground wireless networks.
- 2) We also propose two successive fast positioning (i.e., alternating direction augmented Lagrangian method + conjugate gradient algorithm) for fast and accurate localization.
- 3) We finally evaluate the performance of the proposed algorithms with respect to measurement errors from background noises and underground channel impacts, such as medium conductivity and volumetric water contents.

Simulation results show that the proposed solution achieves *very accurate positioning* in a *very short time* for both low and high noise conditions, as well as under different underground channel settings. Note that the time-efficiency of our algorithm is particularly important for localization in large-scale systems, such as densely-deployed sensor network for oil reservoir monitoring, and for localization with mobile objects, such as people in mines or tunnels.

The remainder of the paper is organized as follows. Section II introduces the related work and Section III presents the system model. Section IV introduces our MI-based localization framework. Under the proposed framework, Section V presents the fast-initial positioning and Section VI presents the fine-grained positioning. Section VII evaluates the localization performance in a practical scenario of randomly-deployed WUSNs and Section VIII concludes the paper.

## II. RELATED WORK

In the literature, the majority of the localization algorithms focus on terrestrial wireless sensor networks. In [13], an overview of localization strategies is provided with the performance evaluation of several existing localization systems. There are three prominent approaches for sensor localization: multidimensional scaling (MDS), simulated annealing (SA), and SDP. Regarding MDS, in [14], a distributed weighted MDS (dwMDS) is proposed that allows a distributed implementation with minimal required communication, accounts for prior location information, and uses a weighted cost function to give heavier weights for accurate pair-wise measurements. In [15], a collaborative localization is given where MDS is used as an initialization method and maximum likelihood estimation further improves the initial results with its fast convergence. However, the drawback of MDS is its high computation complexity and the requirements of much information for its procedures. The poor noise resistance of MDS also makes an additional design a must, limiting its practical usages. In [16], the analysis of flip ambiguities and the robust localization are provided to address the distance measurement errors in centralized SA-based algorithm. However, several critical issues exist in these heuristic-based algorithms, such as the convergence rates, the feasibility to the optimal objective values, signaling exchange overhead, and etc.

In [17], a fast convex relaxation method is employed for a distributed localization implementation that largely depends on the computation capacity of network devices to locally capture an optimal gradient direction of the objective via information broadcasting, which is impossible for WUSNs where the sensors' capabilities and the number of anchors are often very limited. In [11], the convex relaxation technique is applied to transform the non-convex problem into a SDP relaxation for localization with high noisy distance measurements. Instead of employing SDP, another convex relaxation technique, namely the sum of squares (SoS) method, is proposed in [18] that provides highly accurate localization performance at the cost of high computational complexity. Rather than focusing on convex relaxation, a polynomial-time non-convex optimization is further proposed in [19] for

the initial node locations that are sufficient to recover true locations. However, above localization solutions suffer from a poor convergence speed for large-scale networks. The reason is that they do not explore the inherited optimization structure, but simply adopt optimization packages (e.g., SeDuMi in [11]) for their cumbersome problem formulations. In our solution, we intentionally investigate the proposed localization problem and transform our SDP relaxation formulation so that it is solvable via a fast-convergent algorithm, such as ADM [9] that has recently been used to provide a powerful leverage for the algorithm analysis resulted from convex relaxation.

What is more important, all of existing localization solutions fail to address the unique challenges faced by wireless channels in underground environments [20], which will inevitably induce high localization errors if without proper underground channel modeling. Towards this, our proposed localization solution, performed by the data sink, jointly applies ADM and CGA with regards of MI-based communication channel to achieve high positioning accuracy in WUSNs, while maintaining high computational efficiency.

### III. SYSTEM MODEL

First of all, underground localization systems can be classified by the space dimensionality. For example, in Figure 1, mine or tunnel disaster prevention [21] belongs to 1D localization, oil reservoir monitoring [7] needs 2D localization. Specifically, for 1D system in mine or tunnel, the backbone devices are anchors with large loop antennas that mount in tunnels and are apart from each other by a certain distance. Miners carry small MI transceivers to be tracked their positions by the remote control center. For 2D system in reservoir fracture, the anchors are large dipole antennas inside the drilling well to communicate with sensors, which are randomly deployed in an entire oil reservoir. Recently, such in-situ monitoring techniques based on underground sensor networks have drawn lots of attention from the industry and research parties. For example, the small and robust sensors oil reservoir monitoring have been developed [22]. Such micro wireless sensor nodes have been successfully deployed into oil reservoirs [23].

In this paper, we focus on the more challenging 2D localization in oil reservoir environment. Figure 1 shows the typical oil reservoir environment. The wellbore is drilled to the underground oil reservoirs at the depth of around 1.8 [km]. The hydraulic fracturing process utilizes high pressure fluid to generate several long but very narrow fractures, which act as the tunnels between the wellbore and the targeted rock formations. By such a way, the oil and natural gas can be extracted. The fracture generally has the length reaching up to 100 [m] and typically has the width and height of 0.01 [m] and 1 [m], respectively. Since the sensors are injected into the fractures based on hydraulic fracturing process, their locations are fully random. Consider a randomly-deployed WUSNs consisting of  $N$  sensors with random positions denoted by the set  $\{x_i \in \mathbb{R}^2 : 1 \leq i \leq N\}$  and  $K$  anchors with known positions denoted by the set  $\{a_k \in \mathbb{R}^2 : 1 \leq k \leq K\}$ . These anchor locations provide the reference points for other sensors.

In addition, based on the MI channel models (details will be explained in Section IV-A), two types of information are

available to the localization systems. In particular, as shown in Figure 1, the channel models provide the estimated distances among sensors, i.e.,  $\hat{d}_{ij}$ ,  $1 \leq i \leq N$  and  $j \in NH_i$  where  $NH_i$  denote the neighbor set of sensor  $i$ , and between anchors and sensors, i.e.,  $\hat{d}_{ik}$ ,  $1 \leq i \leq N$  and  $1 \leq k \leq K$ , from the respective RMFS. Since anchors can be directly connected to external power sources, they can achieve sufficiently long communication ranges such that the direct communication links exist for each anchor to every sensor, which is different from conventional multi-hop sensor localization problem. As a result, this centralized localization system aims to provide unknown sensor locations from the given anchor locations and the estimated sensor-to-sensor and sensor-to-anchor distances.

### IV. MI-BASED LOCALIZATION FRAMEWORK

We first introduce MI channel modeling and then formulate the MI-based localization framework through the designated cost function and SDP relaxation. The entire framework of the proposed underground localization is shown in Figure 2.

#### A. MI-Based Communication and Channel Model

With MI communication, data information is carried by a time varying magnetic field. Such a magnetic field is generated by a modulated sinusoid current along an MI coil antenna at the transmitter. The receiver retrieves the information by demodulating the induced current along the receiving coil antenna. Since the magnetic field does not exhibit multi-path behavior, given the RMFS, the distance between the transmitter and receiver can be uniquely estimated with regards to AWGN channels in MI-based communication. Specifically, from our previous studies [5], [6], transformer circuit models can be applied to accurately obtain the path loss of MI-based communication, thus providing required estimated distances for localization systems. The details are given in the following.

1) *Distance estimation for MI-based communication:* First of all, based on our MI channels [6], we have

$$10^{P_r/10} = 10^{(P_t - L_{MI})/10} + W, \quad (1)$$

where  $P_r$  [dBm] and  $P_t$  [dBm] are the RMFS and transmitted power, respectively;  $L_{MI}$  [dB] is the path loss;  $W$ , a zero mean Gaussian distributed random variable with standard deviation  $\phi$ , accounts for the background noise. With  $m$  collected RMFS measurements, i.e.,  $P_{r1}, \dots, P_{rm}$ , Eq. (1) implies that these measurements are independent and identically distributed (i.i.d.) Gaussian variable with mean  $\theta$  and variance  $\phi^2$ . Towards this, we can derive the likelihood function  $L(\cdot)$  of mean value  $\theta$ , i.e., RMFS, from  $m$  measurements as

$$L(\theta|P_{r1}, \dots, P_{rm}) = \prod_{i=1}^m \frac{\exp(-(P_{ri} - \theta)^2/2\phi^2)}{\sqrt{2\pi\phi^2}}. \quad (2)$$

Considering the maximum likelihood estimate  $\hat{\theta}_{ML}$ , we have  $\frac{d}{d\theta} \log L(\theta|P_{r1}, \dots, P_{rm})|_{\hat{\theta}_{ML}} = 0$ . This implies that

$$\hat{\theta}_{ML} = \frac{1}{m} \sum_{i=1}^m P_{ri}. \quad (3)$$

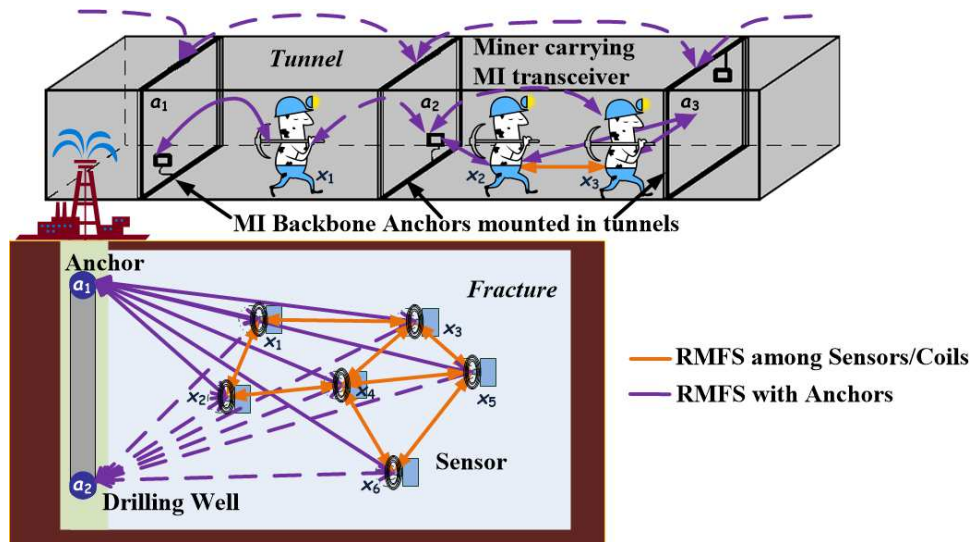


Fig. 1: Randomly-deployed WUSNs for different underground applications: 1D localization in mines or tunnels [21] and 2D localization in oil reservoirs [7].

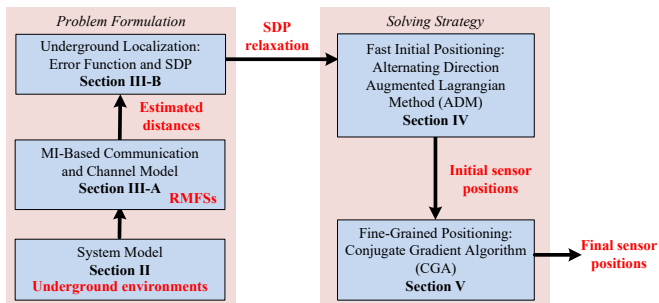


Fig. 2: The entire localization framework for randomly-deployed WUSNs with regard to sections in this paper.

Eq. (3) shows that the maximum likelihood RMFS estimate from  $m$  measurements is the sample mean of collected measurements. With this unbiased estimator  $\hat{\theta}_{ML}$ , the transmission distance  $d$  can be uniquely estimated from the MI path loss model [6] as

$$\hat{d} = \arg \left\{ d \left| \left( 10^{\frac{P_t - \hat{\theta}_{ML}}{10}} - 1 \right) = \frac{16R_0^t(T)R_0^r(T)d^3}{\omega^2 \mu^2(T)N_t N_r a_t^3 a_r^3 G^2(\sigma(T, \varepsilon), \omega, d)} \right. \right\}, (4)$$

where  $\omega$  is the operating angular frequency,  $\mu$  [H/m] the magnetic permeability,  $T$  [°K] the working temperature,  $\varepsilon$  [F/m] the electrical permittivity,  $\sigma$  [S/m] the electrical conductivity,  $G(\cdot)$  an additional loss factor from the skin depth effect,  $N_i$  ( $N_j$ ) number of turns of the transmitter  $i$  (receiver  $j$ ) coil,  $a_i$  ( $a_j$ ) [m] the radius, and  $R_0^i$  ( $R_0^j$ ) [ $\Omega/m$ ] unit length resistance. Note that the estimated distance  $\hat{d}$  in Eq. (4) indicates that as the transmission distance  $d$  increases, RMFS decreases with a rate of  $1/d^3$ . Also, in 2D oil reservoir environments, the angle between the transmitter (receiver) coil radial and the line connecting two coils becomes zero. Last but not the least, this derived MI channel model [5], [6] is validated through several experiments in an underground testbed in our lab [8]. Thus,

by exploiting the unique propagation of multi-path fading free property of MI-based signals, we aim to propose an accurate and fast localization algorithm for underground environments.

### B. Underground Localization: Error Function and SDP

Based on the RMFS-based distance estimation strategy, we formulate the localization framework through an error function and SDP relaxation, which aims to minimize the errors between estimated positions and the actual ones. In other words, we aim to find the sensor positions that minimize the designated error function given the estimated distances in Eq. (4). Towards this, the estimation errors in our localization system are defined as

$$\epsilon_{ij} = \|x_i - x_j\|^2 - \hat{d}_{ij}^2; \quad \epsilon_{ik} = \|x_i - a_k\|^2 - \hat{d}_{ik}^2, \quad (5)$$

where  $\{x_i\}_{1 \leq i \leq N}$  is the set of sensor positions,  $\{a_k\}_{1 \leq k \leq K}$  is the set of anchor positions, and  $\hat{d}_{ij}$  ( $\hat{d}_{ik}$ ) are estimated node-to-node distances, obtained from Eq. (4). Given  $X := [x_1, \dots, x_N]$ , we minimize error function  $f(X)$  to estimate sensor positions (i.e.,  $\hat{X}$ ) as follows. Specifically, we have

$$\begin{aligned} \hat{X} &= \arg \min_X f(X) \\ &:= \arg \min_X \sum_{\{(i,j): 1 \leq i \leq N, j \in NH_i\}} (\|x_i - x_j\|^2 - \hat{d}_{ij}^2)^2 \\ &\quad + \sum_{\{(i,k): 1 \leq i \leq N, 1 \leq k \leq K\}} (\|x_i - a_k\|^2 - \hat{d}_{ik}^2)^2, \quad (6) \end{aligned}$$

where the first portion of  $f(X)$  is from the estimation mismatch among sensors and the second portion of  $f(X)$  is from the mismatch among sensors and anchors. Eq. (6) implies that the error function  $f(X)$ , seen as the  $L_2$  norm of errors from a given guess of  $X$ , is a polynomial function of degree four.

Based on this error function minimization in Eq. (6), we apply the SDP relaxation to obtain the proposed underground localization framework as

$$\begin{aligned}
 \min \quad & \sum_{\{(i,j):1 \leq i \leq N, j \in NH_i\}} \epsilon_{ij}^2 + \sum_{\{(i,k):1 \leq i \leq N, 1 \leq k \leq K\}} \epsilon_{ik}^2 \\
 \text{s.t.} \quad & (0; e_i - e_j)^T Z (0; e_i - e_j) = \epsilon_{ij} + \hat{d}_{ij}^2 \quad \forall (i, j) \\
 & (a_k; -e_i)^T Z (a_k; -e_i) = \epsilon_{ik} + \hat{d}_{ik}^2 \quad \forall (i, k) \\
 & Z = \begin{pmatrix} I & X \\ X^T & Y \end{pmatrix} \succeq 0
 \end{aligned} \quad (7)$$

where the relaxation means that the last equation relaxes from  $Y = X^T X$  to  $Y \succeq X^T X$ , and  $I$  denotes the identity matrix. On the one hand, the SDP relaxation of  $Y \succeq X^T X$  makes the non-convex optimization problem defined in Eq. (7) becomes a convex one, which is easier to solve. On the other hand, the high-rank property of SDP relaxation [24] *lifts* the obtained solution into a higher dimensional space, i.e., higher than  $\mathbb{R}^2$  in Eq. (7), which results in estimation errors. This, in turn, necessitates the design of *rounding* operation to obtain the solution into the correct dimensionality, i.e.,  $\mathbb{R}^2$ .

In the following, we first propose a fast convergent scheme for the problem in Eq. (7) through alternating direction augmented Lagrangian method in Section V, which has controllable computation complexity. After that, we propose a time-efficient search algorithm through conjugate gradient algorithm in Section VI to yield a highly accurate localization solution within  $\mathbb{R}^2$  for randomly-deployed sensors in WUSNs.

#### V. FAST-INITIAL POSITIONING: ALTERNATING DIRECTION AUGMENTED LAGRANGIAN METHOD (ADM)

When the number of constraints of SDP problem approaches the order of unknown parameters, interior point methods [10], as the conventional solutions to SDP problem, become impractical both in terms of computation time and storage at each iteration. On the contrary, ADM [9], a fast first-order method, provides much less computation and storage and could further take advantage of problem structure such as sparsity. Thus, it is more suitable and sometimes the only practical choice for solving large-scale SDPs. In the following, we first examine a specific SDP form of localization problem. We then propose a fast-initial positioning through ADM for the SDP problem. Finally, we analyze the convergence rate to verify fast convergence of the proposed solution.

##### A. Underground Localization SDP Problem

To effectively utilize fast-convergent ADM for solving the localization SDP problem, we need to transform the original SDP in Eq. (7). Specifically, we first reformulate Eq. (7) into a matrix form as follows:

$$\begin{aligned}
 \min \quad & \epsilon^T \epsilon \\
 \text{s.t.} \quad & \langle A_{ij}, Z \rangle = \epsilon_{ij} + \hat{d}_{ij}^2 \quad \forall (i, j) \\
 & \langle \bar{A}_{ik}, Z \rangle = \epsilon_{ik} + \hat{d}_{ik}^2 \quad \forall (i, k) \\
 & Z \succeq 0
 \end{aligned} \quad (8)$$

where  $\epsilon := [\epsilon_{ij}]^T$  denotes the error vector with transpose operation  $T$ , and

$$\begin{aligned}
 A_{ij} &:= \begin{pmatrix} 0 \\ e_i - e_j \end{pmatrix} \begin{pmatrix} 0 & e_i - e_j \end{pmatrix}, \\
 \bar{A}_{ik} &:= \begin{pmatrix} a_k \\ -e_i \end{pmatrix} \begin{pmatrix} a_k & -e_i \end{pmatrix}
 \end{aligned} \quad (9)$$

denote two auxiliary matrices with respect to constraints in Eq. (7). Same as the interpretation of original SDP, in Eq. (8), the objective function aims to minimize mismatch errors from location estimation, and the constraint functions indicate two causes of estimation mismatch as well as the SDP relaxation. Furthermore, we combine the constraints of  $A_{ij}$  and  $\bar{A}_{ik}$  in Eq. (8) into a single constraint as:

$$\begin{aligned}
 A(Z) &:= [\langle A_{ij}, Z \rangle, \langle \bar{A}_{ik}, Z \rangle]^T \\
 &= [\epsilon_{ij} + \hat{d}_{ij}^2, \epsilon_{ik} + \hat{d}_{ik}^2]^T := b(\epsilon)
 \end{aligned} \quad (10)$$

where  $A(Z)$  is a linear map of  $Z$ . Finally, we formulate the underground localization problem as a specific SDP, which can be further solved by ADM [9] in Section V-B, as follows:

$$\begin{aligned}
 \min \quad & \epsilon^T \epsilon \\
 \text{s.t.} \quad & A(Z) = b(\epsilon); Z \succeq 0
 \end{aligned} \quad (11)$$

To optimize sensor localization, we make the following Assumption 1 for localization problem throughout the paper.

**Assumption 1.** *The optimal solution exists for localization in Eq. (7); that is, the matrices  $\{A_{ij}, \bar{A}_{ik}\}_{i,j,k}$  have full row rank and the Slater condition [24] holds for Eq. (11).*

From the above Assumption 1, the existence of optimal solution for sensor localization holds.

##### B. Fast-Initial Positioning through ADM

To solve the SDP problem in Eq. (11), we exploit the widely-adopted ADM framework [25]. However, the framework in [25] cannot be directly applied to our special underground localization formulation, i.e., a specific SDP problem in Eq. (11), without further detailed examinations and derivations. Specifically, first while the analysis in [25] works on the dual problem of the standard SDP, the considered objective function in [25] is linear. However, ours is nonlinear (quadratic) and thus complicates the primal iteration of  $\epsilon$  as indicated by Eq. (14). Second, the constraint related to the semi-definiteness condition is different between [25] and ours. More specifically, in [25], a semi-definite matrix is added to the output of the adjoint operator of linear map  $A^*$  (i.e., addition operations), where  $A^*(y) := \sum_i (\sum_j y_j^j A_{ij} + \sum_k y_k^k \bar{A}_{ik})$  from Eq. (10). However, in our work, the semi-definite matrix  $Z$  is the input of linear map  $A$  (i.e., functional operations), which brings involved iterations of primal  $Z$  and dual  $\Lambda$  as in Eq. (16) and Eq. (17), respectively. In the following, we present an ADM-based, rigorous, and fast-convergent positioning algorithm with the specific SDP formulation in Eq. (11).

First, the transformation from the SDP formulation in Eq. (11) to an augmented Lagrangian function is standard [9], [25] and can be derived as  $L_\rho(Z, \epsilon, \Lambda) = \epsilon^T \epsilon + \langle \Lambda, A(Z) - b(\epsilon) \rangle + \frac{1}{2\rho} \|A(Z) - b(\epsilon)\|_F^2$ , where  $\rho > 0$  is related to the *penalty parameter* and  $\Lambda$  is the dual variable. Next, ADM works with  $L_\rho$  to yield the updating rules of primal and dual variables. Specifically, we solve the problem of  $\min_{\epsilon, Z \succeq 0} L_\rho(Z, \epsilon, \Lambda)$  on the  $m^{\text{th}}$  iteration for  $Z^{m+1}$  and  $\epsilon^{m+1}$ , starting from dual  $\Lambda^0 = \mathbf{0}$ . We then update the dual variable  $\Lambda_{m+1}$  by  $\Lambda^{m+1} = \Lambda^m + \frac{A(Z^{m+1}) - b(\epsilon^{m+1})}{\rho}$ . Moreover, inspired by [25], to avoid time consuming operation of jointly minimizing  $L_\rho$  with primal  $Z$

and  $\epsilon$ , we minimize the augmented Lagrangian function  $L_\rho$  for  $Z$  and  $\epsilon$  iteratively. Specifically, updating rules for primal and dual variables are

$$\epsilon^{m+1} := \arg \min_{\epsilon} L_\rho(Z^m, \epsilon, \Lambda^m); \quad (12a)$$

$$Z^{m+1} := \arg \min_{Z \succeq 0} L_\rho(Z, \epsilon^{m+1}, \Lambda^m); \quad (12b)$$

$$\Lambda^{m+1} := \Lambda^m + \frac{1}{\rho} [A(Z^{m+1}) - b(\epsilon^{m+1})]. \quad (12c)$$

Note that the order of above Eqs. (12a)-(12c) is not relevant as similar convergence results and numerical performance can be yielded through any order [9], [25]. Upon this stage, the proposed SDP relaxation in Eq. (7) is completely solved by this time-efficient updating approach in Eqs. (12a)-(12c).

To further ease the computational complexity of updating rules [25], we exploit several mathematical operations for primal variables  $\epsilon$  and  $Z$ . More specifically, we apply (i) the first-order optimality [10] to Eq. (12a) for an explicit solution and (ii) the eigenvalue decomposition to ease the minimization problem in Eq. (12b). First, we derive the optimality condition for  $\epsilon^{m+1}$  in Eq. (12a) as

$$\begin{aligned} \nabla_{\epsilon} L_\rho(Z^m, \epsilon^{m+1}, \Lambda^m) &= 2\epsilon^{m+1} - \Lambda^m - \frac{1}{\rho} [A(Z^m) - b(\epsilon^{m+1})] \\ &= 0. \end{aligned} \quad (13)$$

Thus, we obtain the updating rule of primal variable  $\epsilon^{m+1} = \epsilon(Z^m, \Lambda^m)$  as

$$\epsilon(Z, \Lambda) = -(2\rho + 1)^{-1} [D - A(Z) - \rho\Lambda], \quad (14)$$

where  $b(\epsilon) = \epsilon + D$  from Eq. (10). As mentioned, Eq. (14) is re-derived because of the nonlinear objective function of our specific SDP formulation in Eq. (11).

Next, regarding  $Z^{m+1}$  in Eq. (12b), we rearrange the terms of  $L_\rho(Z, \epsilon^{m+1}, \Lambda^m)$  and verify that Eq. (12b) is equivalent to

$$\begin{aligned} \min_Z \quad & \|A(Z) - V^{m+1}\|_F^2 \\ \text{s.t.} \quad & Z \succeq 0 \end{aligned}, \quad (15)$$

where  $V^{m+1} := V(\epsilon^{m+1}, \Lambda^m)$  and  $V(\epsilon, \Lambda) := b(\epsilon) - \rho\Lambda$ . Note that the equivalent problem here is different from [25] because of the differences in semi-definiteness conditions. Also, let  $U^{m+1} = (A^*A)^{-1}A^*(V^{m+1})$  with the adjoint operator  $A^*$ , and  $A^*A$  is invertible from Assumption 1. By the eigenvalue decomposition, we thus obtain the explicit solution of the updating rule of primal variable  $Z^{m+1}$  as

$$Z^{m+1} = U_{\ddagger}^{m+1} = P_{\ddagger} \Sigma_{+} P_{\ddagger}^T \quad (16)$$

(i.e.,  $P\Sigma P^T$  is the spectral decomposition of the matrix  $U^{m+1}$  with nonnegative  $\Sigma_{+}$  and negative  $\Sigma_{-}$  eigenvalues. Moreover, we can reexamine the updating rule in Eq. (12c) as follows:

$$\Lambda^{m+1} = \frac{A(Z^{m+1}) - V^{m+1}}{\rho}. \quad (17)$$

It implies that  $A^*(\Lambda^{m+1}) = \frac{1}{\rho}(A^*A)(Z^{m+1} - U^{m+1}) = \frac{1}{\rho}(A^*A)(U_{\ddagger}^{m+1})$ , where  $U_{\ddagger}^{m+1} := -P_{\ddagger} \Sigma_{-} P_{\ddagger}^T$  and can be solved in polynomial-time from a simple linear matrix inequality (LMI). Specifically, while the generic work in [25] has a direct implication, our LMI involves both linear mapping and

adjoint operator. With the above accomplishments, we propose the ADM-based fast-initial positioning in **Algorithm 1**.

---

**Algorithm 1:** ADM-Based Fast-Initial Positioning

---

**Input :**  $(A_{ij}, \bar{A}_{ik}), (\hat{d}_{ij}^2, \hat{d}_{ik}^2)$   
 $1 \leq i \leq N, j \in NH_i, 1 \leq k \leq K$

**Output:**  $x_i, 1 \leq i \leq N$

- 1 **Initialize** primal  $Z^0 \succeq 0$  and dual  $\Lambda^0 \succeq 0$
  - 2 **for**  $m = 0, 1, \dots$  **do**
  - 3     **Calculate**  $\epsilon^{m+1}$  from Eq. (14)
  - 4     **Calculate**  $V^{m+1}, U^{m+1}$ , eigenvalue decomposition of  $U^{m+1}$ , and  $Z^{m+1}$  from Eq. (16)
  - 5     **Calculate**  $\Lambda^{m+1}$  from Eq. (17)
  - 6 **end**
- 

### C. Convergence Analysis of Algorithm 1

In this section, we perform the convergence analysis, which shows that **Algorithm 1** converges fast towards the optimal solutions. In particular, we first (i) prove the algorithm is globally convergent and then (ii) show that the algorithm converges to the optimal solutions at rate  $O(1/m)$ .

**Theorem 1. [Global Convergence of Algorithm 1.]** *Let  $\mathcal{Z}$  denote the set of primal and dual solutions for the primal problem in Eq. (11) and the corresponding dual problem. Then, from any starting point  $(Z^0, \epsilon^0, \Gamma^0(\Lambda^0))$  where  $\Gamma^{m+1} := (A^*A)^{-1}A^*(\Lambda^{m+1})$ , **Algorithm 1** achieves the convergence of sequence  $\{(Z^m, \epsilon^m, \Gamma^m(\Lambda^m))\}$  to a set solution  $(Z^*, \epsilon^*, \Gamma^*(\Lambda^*)) \in \mathcal{Z}$ .*

Theorem 1 shows the global convergence of **Algorithm 1**, which implies that the proposed iterative method converges for an arbitrary initial approximation. The proof of Theorem 1 is based on a similar fixed-point argument [25] with regards to our specific localization formulation in Eq. (11). To simplify the readability of this paper, the details of the proof can be found in our technical report [26, Appendix A].

In addition, because of the difference in problem formulations, we cannot directly apply the convergence speed analysis of the generic SDP problems in [25] for our specific SDP problem. This is mainly because the convergence of the dual variables in our algorithm is not straight-forward as that in [25]. In particular, the convergence of dual part in Theorem 1 involves a derived function of dual variables, i.e.,  $\Gamma(\Lambda) = (A^*A)^{-1}A^*(\Lambda)$ , while the work in [25] only deals with the dual variables themselves. Hence, we analyze the convergent rate of **Algorithm 1** as follows.

**Theorem 2. [Global Linear Convergence of Algorithm 1.]** *Let  $W^m = \|U^m - U^*\|_F^2$  and  $D^m = \|U^{m+1} - U^m\|_F^2$ . Under the same assumption of Theorem 1,  $D^m$  is non-increasing and  $D^m \leq W^0/(m+1)$  for all  $m$ . That is, **Algorithm 1** has an  $O(1/m)$  rate of convergence.*

The key ideas of proving Theorem 2 are (i) examining the relationship between primal, dual infeasibility and the difference between matrices  $\{U^m\}$  from Section V-B and (ii)

using the Saddle Point Theorem [24] and Assumption 1, the Lyapunov function  $W^m$ , and the nonincreasing  $D^m$  to address linear convergence. Again in order to simplify the readability of this paper, the details of the proof can be found in our technical report [26, Appendix B].

## VI. FINE-GRAINED POSITIONING: CONJUGATE GRADIENT ALGORITHM (CGA)

As mentioned in Section IV-B, the solution obtained from SDP relaxation has the high-rank property. For example, in 2D oil reservoir, the high-rank optimal solution from the proposed ADM should be translated into 2D location solution without losing the optimality. In other words, we can fine-tune the sensor positioning to further increase the location accuracy, based on the results of fast-initial positioning. This idea is easily realized through the design of search algorithm for the optimal location solution in the correct dimensionality. In the following, we first examines the straightforward method, steepest descent (SD), which utilizes the gradient of objective function for searching the minimum. Then, we apply a more sophisticated search approach based on the conjugate gradient algorithm, which exploits conjugate direction (CD) to outperform the conventional steepest descent method [10].

### A. Steepest Descent (SD) Method

The objective function in Eq. (6) of the localization problem is first reformulated as

$$f(X) = \sum [d_{ij}^2 - (x_i - x_j)^T(x_i - x_j)]^2 + \sum [d_{ik}^2 - (x_i - a_k)^T(x_i - a_k)]^2. \quad (18)$$

Define  $\nabla f$  as  $\nabla f(X) = [Df_{x_1}, \dots, Df_{x_n}]^T$  where  $Df_{x_i} = [\frac{\partial f}{\partial x_i^1}, \frac{\partial f}{\partial x_i^2}]$  for 2D cases. Note that,  $\nabla f$  is the decent direction of the objective function in Eq. (18). The SD method [10] provides that given  $X^{(0)}$ , the search iteration follows

$$\begin{aligned} X^{(m+1)} &= X^{(m)} - \alpha_m \nabla f(X^{(m)}) \\ \alpha_m &= \arg \min_{\alpha \geq 0} f(X^{(m)} - \alpha \nabla f(X^{(m)})) \end{aligned} \quad (19)$$

where  $\alpha_m$  is the step size of the  $(m+1)^{th}$  iteration. In other words, it performs an exact line-search to decide the step size to minimize  $f(X^{(m+1)})$  along the  $\nabla f(X^{(m)})$  direction. Hence, the optimal step size  $\alpha_m$  of the  $(m+1)^{th}$  iteration is obtained through the following equation

$$\left. \frac{df(X^{(m)} - \alpha \nabla f(X^{(m)}))}{d\alpha} \right|_{\alpha=\alpha_m} = 0. \quad (20)$$

As suggested by [11],  $\alpha_m$  can be further obtained from Eq. (18) and Eq. (20) by  $4c_1^2\alpha_m^3 + 6c_1c_2\alpha_m^2 + 2(c_2^2 + 2c_1c_3)\alpha_m + 2c_2c_3 = 0$ , where  $c_1 = -\sum_i Df_{x_i^{(m)}} Df_{x_i^{(m)}}^T$ ,  $c_2 = -2\sum(x_i^{(m)} - x_j^{(m)})Df_{x_i^{(m)}} - 2\sum(x_i^{(m)} - a_k)Df_{x_i^{(m)}}$ , and  $c_3 = \sum[d_{ij}^2 - (x_i^{(m)} - x_j^{(m)})^T(x_i^{(m)} - x_j^{(m)})] \sum[d_{ik}^2 - (x_i^{(m)} - a_k)^T(x_i^{(m)} - a_k)]$ . Note that the derived equation for  $\alpha_m$  here is a third order polynomial and the analytical solution of roots thus exists. Also, a widely-used Armijo rule [27] can alternatively serve as a good approximation of the step size.

Through the above gradient-based search, we are able to round the high-dimensional (rank) solution from the proposed ADM to the desired dimensionality of sensor location. In the following, we introduce a more sophisticated search that achieves optimal points much faster than the steepest descent method and avoids possibly being stuck in local optima.

### B. CGA with Conjugate Direction (CD)

The basic concept of the conjugate gradient algorithm [10] is to minimize the objective function, e.g.,  $f(X)$  in Eq. (18), along with the corresponding conjugate direction (CD) of each iteration, e.g.,  $d^{(0)}$  and  $d^{(m+1)}$ ,  $m \geq 0$  in Eq. (22), instead of adhering to the gradient direction, like in the steepest descent method. Specifically, rather than adopting Eq. (19) in each iteration, the CGA provides that given  $X^{(0)}$ , the search iteration follows

$$X^{(m+1)} = X^{(m)} + \alpha_m d^{(m)} \quad (21)$$

where  $d^{(0)} = -\nabla f(X^{(0)})$  applies the gradient direction for the first iteration and the step size  $\alpha_m$  is determined by  $\alpha_m = \arg \min_{\alpha \geq 0} \Phi_m(\alpha)$  where  $\Phi_m(\cdot)$  is defined as  $\Phi_m(\alpha) := f(X^{(m)} + \alpha d^{(m)})$ . If CGA does not approach the minimum point after the current iteration, it constructs the next CD  $d^{(m+1)}$  from the current direction  $d^{(m)}$  by

$$d^{(m+1)} = -\nabla f(X^{(m+1)}) + \beta_m d^{(m)} \quad (22)$$

where  $\beta_m$  is obtained via the conjugate concept by Fletcher-Reeves [10] as  $\beta_m = \frac{\|\nabla f(X^{(m+1)})\|^2}{\|\nabla f(X^{(m)})\|^2}$ . In other words, the parameter sets of  $(\alpha_m, \beta_m)_{m \geq 0}$  are obtained as

$$\begin{aligned} \alpha_m &= \arg \min_{\alpha \geq 0} f(X^{(m)} + \alpha d^{(m)}); \\ \beta_0 &= \frac{\sum_i Df_{x_i^{(1)}} Df_{x_i^{(1)}}^T (e_i - \alpha_0 F_i)^T (e_i - \alpha_0 F_i)}{\sum_i Df_{x_i^{(0)}} Df_{x_i^{(0)}}^T}; \\ \beta_m &= \frac{\nabla f(X^{(m+1)})^T \nabla f(X^{(m+1)})}{\nabla f(X^{(m)})^T \nabla f(X^{(m)})}, \end{aligned} \quad (23)$$

where  $e_i = [\mathbf{0}^{1 \times 2}, \dots, \mathbf{0}^{1 \times 2}, \mathbf{1}^{1 \times 2}, \mathbf{0}^{1 \times 2}, \dots, \mathbf{0}^{1 \times 2}]^T$  and  $F_i = [D_{x_i^{(m)}} Df_{x_1^{(m)}}, \dots, D_{x_i^{(m)}} Df_{x_i^{(m)}}, \dots, D_{x_i^{(m)}} Df_{x_n^{(m)}}]^T$ . Finally, the CGA is proposed in **Algorithm 2** for the fine-grained positioning. To this end, we completely solve the underground localization with randomly-deployed sensors through the successive execution of the proposed ADM in **Algorithm 1** and CGA in **Algorithm 2**.

## VII. PERFORMANCE EVALUATION IN OIL RESERVOIRS

We evaluate the proposed MI-based localization solution (i.e., **Algorithm 1**: ADM + **Algorithm 2**: CGA) in a practical scenario of 2D oil reservoirs. Simulation results confirm that our solution achieves great positioning accuracy and functions well even under severe environmental impact in terms of volumetric water content, favored by the practical implementation in randomly-deployed WUSNs. In the following, we first evaluate two proposed successive algorithms in 2D oil reservoir fractures. Then, we examine the underground environmental impact in the localization performance.

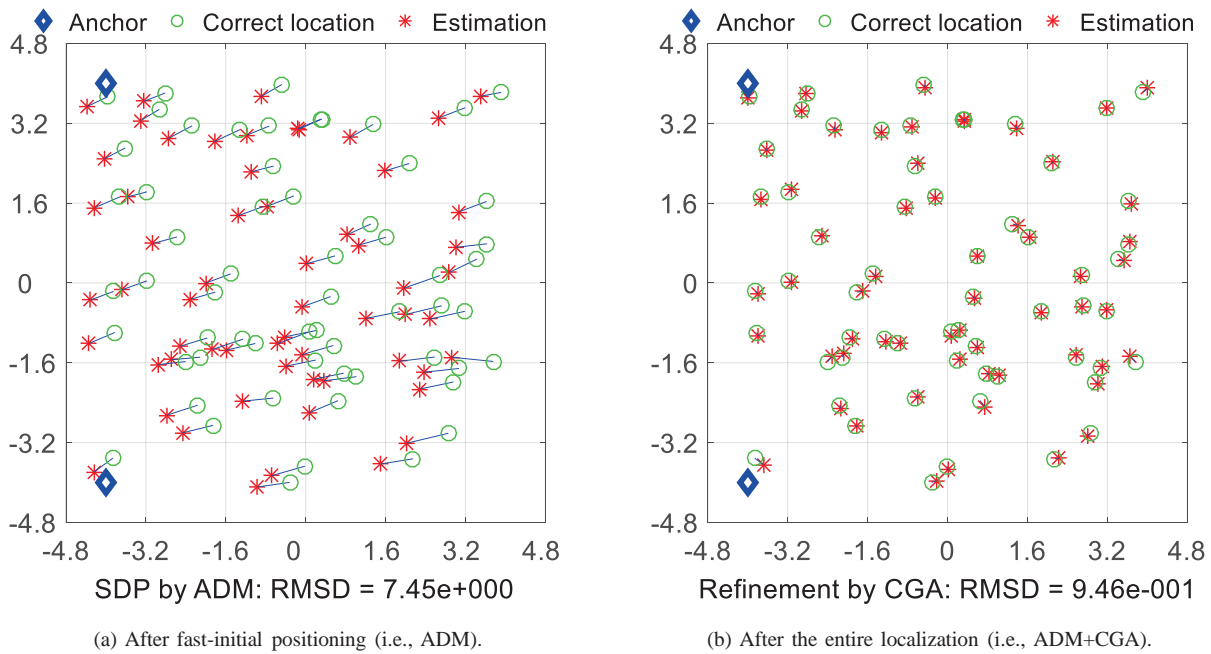


Fig. 3: Localization results for 60 sensors with  $nf=1$ .

**Algorithm 2: CGA (Fine-Grained Positioning)**

**Input :**  $f(\cdot)$  from Eq. (18),  $X^{(0)} := [x_1^T, \dots, x_N^T]^T$  from **Algorithm 1**  
**Output:**  $X^*$  % Sensor location

- 1 **Set**  $m = 0$ ; **compute**  $d^{(0)} = -\nabla f(X^{(0)})$
- 2 **while**  $\nabla f(X^{(m)}) \neq \mathbf{0}$  **do**
- 3     **Compute**  $\alpha_m$  according to Eq. (23)
- 4     **Compute**  $X^{(m+1)}$  according to Eq. (21)
- 5     **Compute**  $\beta_m$  according to Eq. (23)
- 6     **Compute**  $d^{(m+1)}$  according to Eq. (22)
- 7     **Set**  $m = m + 1$
- 8 **end**
- 9 **Set**  $X^* = X^{(m)}$

A. 2D Localization in Oil Reservoir Fractures

As shown in Figure 1, it is assumed that there are two anchors inside a single drilling well and sensors are randomly spread in a two-dimensional fracture. All simulation parameters and values are given in Table I, with regard to realistic oil reservoirs. Particularly, it is considered that each anchor has the direct communication link to every sensor from its larger transmission range and coil antenna parameters are set to fit in the thin-width fracture. In addition, to characterize the noise level from the estimation errors, noise factor ( $nf$ ) is defined as  $\hat{d}_{ij} = d_{ij}(1 + N(0, 1) \times nf)$ , which is a given number between  $[0, 1]$  to control the amount of noise variance. Moreover, to characterize the positioning accuracy by measuring the estimation mismatch, the root-mean-square distance (RMSD) metric is further defined as  $RMSD = \frac{1}{\sqrt{N}} \left( \sum_{i=1}^N \|x_i - \hat{x}_i\|^2 \right)^{1/2}$ , where  $x$  is the actual sensor location and  $\hat{x}$  is the one obtained from the localization algorithm.

Figure 3 shows the localization results of 60 unknown sensor locations under high noise level ( $nf=1$ ) after fast-initial positioning (i.e., ADM) and after the entire localization (i.e., ADM+CGA), respectively. Two anchors are marked as blue diamonds at  $[-4, 4]$  and  $[-4, -4]$ . Green circles refer to the original locations of unknown sensors; red asterisks refer to their estimated positions. In Figure 3a, while the estimated positions deviate a little from the actual locations after initial positioning by **Algorithm 1**, this step does not require long processing time, i.e., only few iterations, to obtain the useful results. In Figure 3b, more accurate locations are further obtained by executing fine-grained positioning by **Algorithm 2**. It reduces the estimation errors in RMSD and enhances the localization accuracy with a fast search algorithm. Similar outcomes can be observed in Figure 4 for the larger size of 100 unknown sensor locations. Initial positioning provides rough locations with fast processing time in Figure 4a, and fine-grained positioning further enhance the performance via a powerful and time-efficient search as shown in Figure 4b. The above detailed evaluation confirms that the proposed localization performs well in high noise levels and is indifferent for network sizes through the fast and accurate operations of two successive positioning. Note that Figures 3a-4a indicate that after fast-initial localization, the error vectors of the estimated locations seem to follow the east-west (i.e., horizontal) direction. This biased estimation comes from the very limited two anchors with the following peculiarities in oil reservoirs: (1) the strong impacts from direct transmissions of anchors and (2) the same horizontal axis for the two anchors. Specifically, in practical setups of oil reservoirs (in Figure 1 and [7]), due to the accessibility of the external power sources, anchors achieve longer communication ranges and have direct links to each sensor. Hence, compared to that of short-range transmissions between some paired sensors, the

TABLE I: SIMULATION PARAMETERS AND VALUES FOR PERFORMANCE EVALUATIONS.

Parameters	Values
Fracture area	$8 \times 8$ [m <sup>2</sup> ]
Fracture depth	1.8 [km]
Fracture width	0.03-0.04 [m]
Underground temperature ( $T$ )	418 [°K]
Soil makeup	30% sand particle; 20% clay particle
Bulk density	$1.5 \times 10^6$ [grams/m <sup>3</sup> ]
Solid soil particle density	$2.66 \times 10^6$ [grams/m <sup>3</sup> ]
Magnetic material	30% paramagnetic composites; 10% ferromagnetic composites
MI operating frequency ( $\omega/2\pi$ )	7 [MHz]
Coil antenna radius ( $a$ )	0.01 [m]
Coil antenna turn ( $N$ )	10 turns
Antenna unit-length resistance ( $R_0$ )	0.01 [ $\Omega$ /m]
Sensor's maximum transmission range ( $R$ )	3.2 [m]

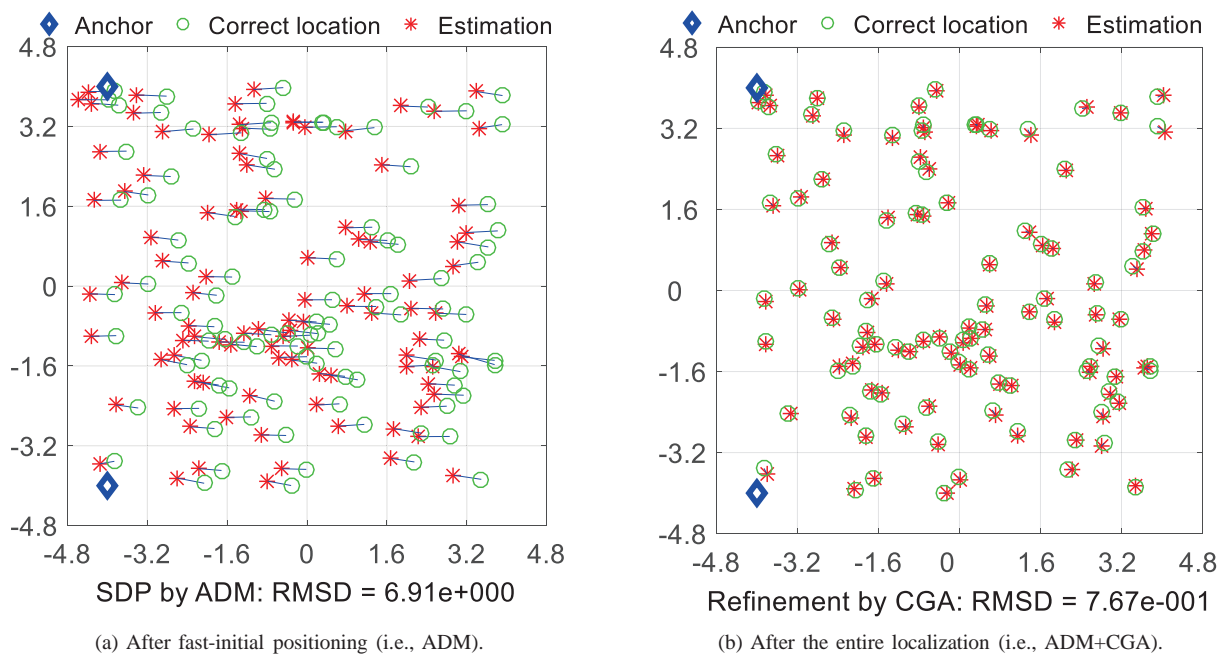


Fig. 4: Localization results for 100 sensors with  $nf=1$ .

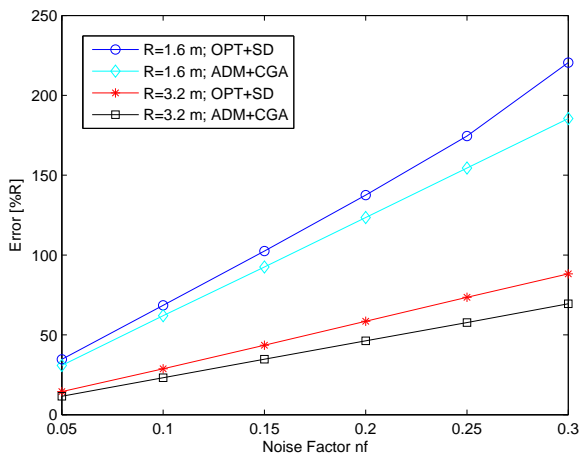
estimated distances (as inputs of our localization systems) of these direct transmissions (between anchors and sensors) have strong impacts and play dominant roles in localization results, especially for limited sensors' transmission ranges. Furthermore, given that the possible anchors only come from the large dipole antenna inside the drilling well, the two anchors will be vertically separated and have the same horizontal location. This implies that the fast-initial positioning is much easier to locate sensors' vertical locations than their horizontal locations, and thus the estimated sensor locations incline to have larger horizontal estimation errors.

Next, in Figure 5, we compare the proposed solution (i.e., ADM+CGA) with the benchmark scheme that combines the conventional SDP solver and steepest decent method (i.e., OPT+SD). Figure 5a shows the performance comparison with 60 sensors in low noise regime. The estimation error is calculated as a percentage of sensors' maximum transmission

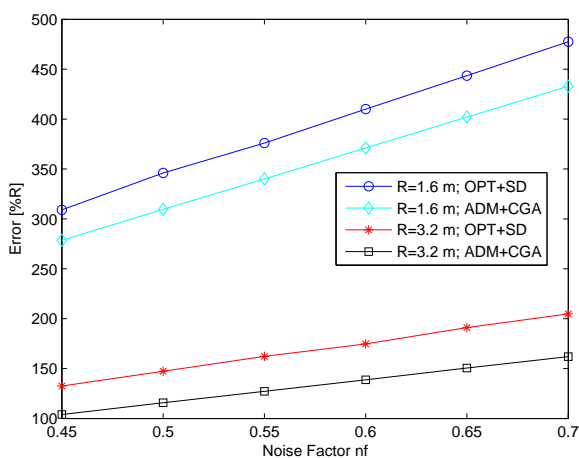
ranges. For both cases of maximum transmission ranges 1.6 [m] and 3.2 [m], the proposed solution has less estimation error than the other under all evaluated noise factors. Two solution has close performance under very low noise ( $nf=0.05$ ). Furthermore, Figure 5b shows the corresponding results in high noise regime. The proposed solution outperforms the other and maintains noticeable performance improvement along the different noise factors. In summary, these results verify the superior design of the proposed localization, facilitating an accurate and time-efficient localization algorithm in randomly-deployed WUSNs.

### B. Underground Environmental Impact

While the MI-based communication is adopted for its suitability in underground, water content in the surrounding areas greatly affects the communication quality. In particular, if



(a) In low noise regime.



(b) In high noise regime.

Fig. 5: Comparison between our solution (i.e., ADM+CGA) and the designated algorithm (i.e., OPT+SD) for 60 sensors.

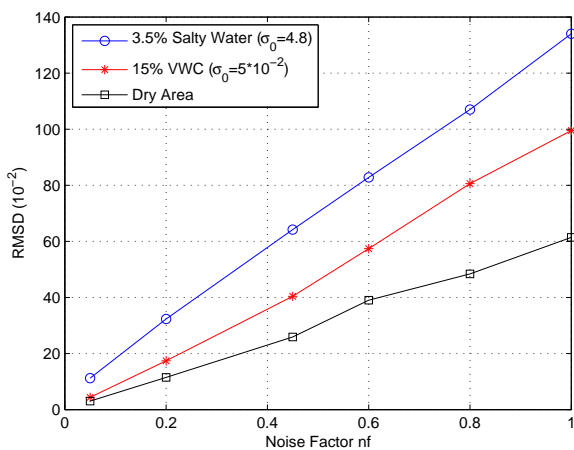


Fig. 6: Conductivity impact on localization results of our solution in oil reservoir environment.  $\sigma_0$  is the electrical conductivity at 293 [°K].

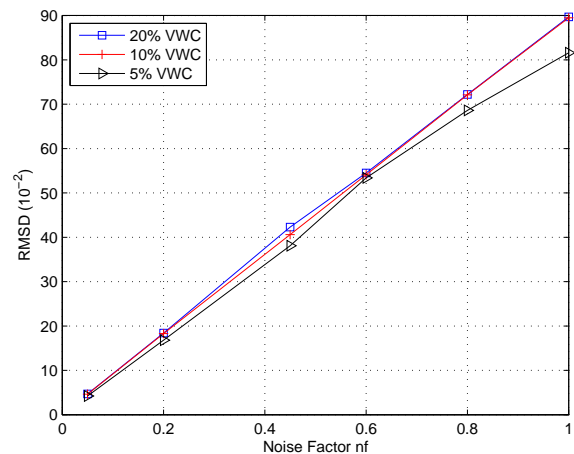


Fig. 7: VWC impact on the localization performance of our solution in oil reservoir environments.

there are more electrolytes in the environments, the induction-based communication and thus the MI-based localization will be dramatically degraded. 60 sensors are randomly-deployed in oil reservoir, and each sensor can tolerate the maximum path loss as 120 [dB]. Figure 6 shows the environmental impact of the electrical conductivity that stems from different water contents. The salty water provides great signal conductivity, impairs the signal induction, and thus gives the worst RMSD values. Moreover, when the noise level is extremely low, i.e.,  $nf=0.05$ , the localization result of 15% volumetric water content (VWC) can approach the one in dry area. However, when the noise becomes larger, the performance difference also increases between the wet and dry areas. In addition, by focusing on the normal water content with conductivity  $\sigma_0 = 5 \times 10^{-2}$ , Figure 7 shows the impact on localization from different volumes of water content. The results show that although the VWC increases, the performance difference is not obvious until in a very high noise levels. Larger VWC brings more signal conductivity than induction and damages the communication and thus the localization performance. With these accomplishments, we successfully bring a fast and accurate MI-based localization that outperforms the existing benchmark and suits the urgent positioning need of randomly-deployed sensors in underground environments.

## VIII. CONCLUSION

In this paper, the fundamental localization challenge in randomly-deployed WUSNs is addressed by exploiting RMFS measurements from MI-based communication and proposing fast and accurate successive positioning algorithms. Leveraging the multi-path and fading free natures of the MI-based communication, RMFS from AWGN channel modeling serves as the location-dependent information for localization algorithm designs. Moreover, the fast ADM provides useful initial positioning within few iterations, and the powerful CGA refines initial results into highly accurate sensor positions. Performance evaluation confirms that the proposed localization

guarantees considerable positioning accuracy with great time-efficiency in underground environments, bringing a novel paradigm for underground sensor localization.

## REFERENCES

- [1] I. F. Akyildiz and E. P. Stuntebeck, "Wireless underground sensor networks: Research challenges," *Ad Hoc Networks (Elsevier)*, vol. 4, no. 6, pp. 669–686, Nov. 2006.
- [2] I. F. Akyildiz, Z. Sun, and M. C. Vuran, "Signal propagation techniques for wireless underground communication networks," *Physical Commun. J.*, vol. 2, no. 3, pp. 167–183, Sep. 2009.
- [3] J. J. Sojdehei, P. N. Wrathall, and D. F. Dinn, "Magneto-inductive (MI) communications," in *2001 MTS/IEEE Conference and Exhibition*, vol. 1, Nov. 2001, pp. 513–519.
- [4] R. Bansal, "Near-field magnetic communication," *IEEE Antennas Propag. Mag.*, vol. 46, no. 2, pp. 114–115, Apr. 2004.
- [5] S.-C. Lin, I. F. Akyildiz, P. Wang, and Z. Sun, "Distributed cross-layer protocol design for magnetic induction communication in wireless underground sensor networks," *IEEE Trans. Wireless Commun.*, vol. 14, no. 7, pp. 4006–4019, Jul. 2015.
- [6] Z. Sun and I. F. Akyildiz, "Optimal deployment for magnetic induction-based wireless networks in challenged environments," *IEEE Trans. Wireless Commun.*, vol. 12, no. 3, pp. 996–1005, Mar. 2013.
- [7] H. Guo and Z. Sun, "Channel and energy modeling for self-contained wireless sensor networks in oil reservoirs," *IEEE Trans. Wireless Commun.*, vol. 13, no. 4, pp. 2258–2269, Apr. 2014.
- [8] X. Tan, Z. Sun, and I. F. Akyildiz, "Wireless underground sensor networks: MI-based communication systems for underground applications," *IEEE Antennas Propag. Mag.*, vol. 57, no. 4, pp. 74–87, Aug. 2015.
- [9] S. Boyd, N. Parikh, E. Chu, B. Peleato, and J. Eckstein, "Distributed optimization and statistical learning via the alternating direction method of multipliers," *Found. Trends Mach. Learn.*, vol. 3, no. 1, pp. 1–122, 2011.
- [10] E. K. P. Chong and S. H. Zak, *An Introduction to Optimization*. Wiley-Sons, 3rd ed., 2008.
- [11] P. Biswas, T. Liang, K. Toh, T. Wang, and Y. Ye, "Semidefinite programming approaches for sensor network localization with noisy distance measurements," *IEEE Trans. on Automation Science and Engineering*, 2006.
- [12] J. F. Sturm, "Using SeDuMi 1.02, a Matlab toolbox for optimization over symmetric cones," *Optim. Methods Softw.*, vol. 11, pp. 625–653, 1999.
- [13] E. Niewiadomska-Szynkiewicz, "Localization in wireless sensor networks: Classification and evaluation of techniques," *International Journal of Applied Mathematics and Computer Science*, vol. 22, no. 2, pp. 281–297, Jun. 2012.
- [14] J. A. Costa, N. Patwari, and A. O. H. III, "Distributed weighted-multidimensional scaling for node localization in sensor networks," *ACM Trans. Sen. Netw.*, vol. 2, no. 1, pp. 39–64, Feb. 2006.
- [15] X. Li, "Collaborative localization with received-signal strength in wireless sensor networks," *IEEE Trans. Veh. Technol.*, vol. 56, no. 6, pp. 3807–3817, Nov. 2007.
- [16] A. Kannan, B. Fidan, and G. Mao, "Analysis of flip ambiguities for robust sensor network localization," *IEEE Transactions on Vehicular Technology*, vol. 59, no. 4, pp. 2057–2070, May 2010.
- [17] C. Soares, J. Xavier, and J. Gomes, "Simple and fast convex relaxation method for cooperative localization in sensor networks using range measurements," *IEEE Trans. Signal Process.*, vol. 63, no. 17, pp. 4532–4543, Sep. 2015.
- [18] J. Nie, "Sum of squares method for sensor network localization," *Computational Optimization and Applications*, vol. 43, no. 2, pp. 151–179, 2009.
- [19] S. Ji, K.-F. Sze, Z. Zhou, A.-C. So, and Y. Ye, "Beyond convex relaxation: A polynomial-time non-convex optimization approach to network localization," in *2013 Proceedings IEEE INFOCOM*, Apr. 2013, pp. 2499–2507.
- [20] S.-C. Lin, I. F. Akyildiz, P. Wang, and Z. Sun, "Optimal energy-throughput efficiency for magneto-inductive underground sensor networks," in *2014 IEEE International Black Sea Conference on Communications and Networking (BlackSeaCom)*, May 2014, pp. 22–27.
- [21] Z. Sun and I. F. Akyildiz, "Channel modeling and analysis for wireless networks in underground mines and road tunnels," *IEEE Transactions on Communications*, vol. 58, no. 6, pp. 1758–1768, Jun. 2010.
- [22] D. Chapman and W. Trybula, "Meeting the challenges of oilfield exploration using intelligent micro and nano-scale sensors," in *2012 12th IEEE Conference on Nanotechnology (IEEE-NANO)*, Aug 2012, pp. 1–6.
- [23] PTRC-INCAS<sup>3</sup> Innovation Centre, "Micro sensor motes successfully travel through a canadian heavy oil reservoir," Tech. Rep., Nov. 2012.
- [24] S. Boyd and L. Vandenberghe, *Convex Optimization*. Cambridge Univ. Press, 2004.
- [25] Z. Wen, D. Goldfarb, and W. Yin, "Alternating direction augmented lagrangian methods for semidefinite programming," *Mathematical Programming Computation*, vol. 2, no. 3–4, pp. 203–230, 2010.
- [26] S.-C. Lin, A. A. Alshehri, P. Wang, and I. F. Akyildiz, "Magnetic induction-based localization in rarandom-deployed wireless underground sensor networks," BWN Lab, the School of ECE, Georgia Institute of Technology, Tech. Rep. [Online]. Available: <http://www.prism.gatech.edu/~sclin88/publications/MLocReport.pdf>
- [27] J. Nocedal and S. J. Wright, *Numerical Optimization*. Springer Series in Operations Research. New York: Springer-Verlag, 1999.